Senior Thesis
Astrophysics Program
California Institute of Technology

David Vartanyan
Advisor: Christian Ott
Date: May 16, 2014

Abstract

Contents

1 Introduction

1.1 LGRB-SN Connection

1.2 Magnetar Model

1.3 Collapsar Model

2 Magnetar Spindown as a Source of GRB Engine Power

We explore the fundamental physics of magnetar spindown as it relates to both the prompt emission and the afterglow phases of the LGRB light curve. In Section 2.1, we introduce the magnetization parameter σ, relevant for our subsequent discussion of the prompt emission energetics and duration. In Section 2.2, we will then derive the dipole model for magnetarspindown which will be relevant for our discussion of afterglow plateaus. Finally, in Section 2.3, we will follow Piro and Ott 2011 [1] to account for possible fallback accretion onto our magnetar. This may affect both prompt emission and afterglow energetics and duration by modifying the magnetization parameter and the magnetar period.

2.1 Magnetization

The magnetization parameter is defined as

$$\sigma_o = \frac{\phi^2 \Omega^2}{\dot{M} c^3} \ , \tag{1}$$

where ϕ is the poloidal magnetic flux, Ω is the angular frequency, and $\dot{M}$ is the mass loss (or possibly mass accretion) rate. We note, as in Piro and Ott 2010 [1], that higher order magnetic poles may be signicant near the magnetar but decay faster than the dipole field, which scales as $1/r^3$, and so became insignificant at larger radii where LGRB prompt emission and afterglow occur.

Naively, we can think of magnetization as a ratio of magnetic field energy density to mass energy density. As will be discussed in Section 3, the magnetization parameter increases drastically on a timescale of $20 - 100\,\mathrm{s}$, during which the neutron star becomes optically thin to neutrinos and consequently $\dot{M}$ declines. This timescale constrains the prompt emission duration since jets with high magnetization cannot effectively accelerate and dissipate their energy [2]. Instead, most of the available rotational energy of the neutron star would remain as a Poynting flux rather than thermalizing to produce emission [2]. The transparency timescale is tauntingly similar to the duration of typical LGRBs of ~ 100 seconds. Metzger et al. [2] cite $30 - 100$s for this timescale, which is a stiff function of opacity and highly sensitive to the interior temperature of the neutron star. We search for physical processes that may decrease the magnetization. Barring decreasing the magnetix flux or the angular frequency, which would also counterproductively decrease the spindown energy, or increasing the speed of light, which stubbornly chooses to remain constant, we are left with increasing $\dot{M}$. Then, the pressing question is whether mass accretion, and not just mass loss, can affect magnetization.

2.2 Magnetar Dipole Radiation

We model magnetar spindown similarly to pulsars and assume a magnetic dipole toy model. The dipolar magnetar field is:

$$B(\vec{r}) = \frac{3\vec{n}(\vec{m}.\vec{n}) - \vec{m}}{r^3}, \tag{2}$$

where $\vec{m}$ is the magnetic moment and $\vec{n}$ is the unit radial vector.

In analogy with Larmor's formula for electric dipole radiation, a time-dependent magnetic dipole radiates

$$\frac{dW}{dt} = -\frac{2}{3c^3} |\ddot{\vec{m}}_\perp|^2, \tag{3}$$

where $\vec{m_\perp}$ is the component of $\vec{m}$ perpendicular to rotation axis.

Defining the angle between the rotation axis and the magnetic dipole moment as α,

$$\vec{m}_\perp = m_o \sin(\alpha) e^{-i\Omega t}, \tag{4}$$

so $|\ddot{\vec{m}}|_\perp^2 = {m_o}^2 \sin\alpha^2 \Omega^4$ since $m_o = BR^3/2$ for a uniformly magnetized sphere.

It follows that the time-averaged dipole radiation is

$$\frac{dW}{dt} = -\frac{{B_p}^2 R^6}{6c^3} \Omega^4 \sin^2\alpha, \tag{5}$$

The larger the angular separation α of the magnetic and rotational axes is, the greater the dipole radiation will be. If we assume the magnetic dipole is oriented perpendicularly to the rotation axis so $\alpha = \pi/2$, the luminosity is powered by spin-down. We define the magnetar spin period $P = 2\pi/\Omega$ and arrive at Eq. 2 from Lyons et al. 2009 [3]

$$L = 9.62065 \times 10^{48}\, B_{p,15}^2 P_{-3}^{-4} R_6^6 \,\mathrm{erg\,s^{-1}}, \tag{6}$$

where $B_{p,15} = B_p/10^{15}\,\mathrm{G}$, $P_{-3} = P/10^3\,\mathrm{s}$, and $R_6 = R/10^6\,\mathrm{km}$.

Next we assume dipole radiation taps the rotational energy of the magnetar, so $\frac{dE_{rot}}{dt} = \frac{dW}{dt}$ where $E_{rot} = 1/2 I w^2$ so $\ddot{E}_{rot} = I\omega\ddot{\omega}$. Define a characteristic dipole spindown time τ_{dipole} as

$\tau_{\mathrm{dipole}} = -\omega/\ddot{\omega}$ It follows that

$$\tau_{\mathrm{dipole}} = \frac{3c^3 I}{{B_p}^2 R^6 \omega^6}, \tag{7}$$

Then,

$$\tau_{\mathrm{dipole}} = 2051.75\ I_{45} B_{15,p}^{-2} P_{-3}^2 R_6^{-6}\,\mathrm{s}, \tag{8}$$

which is equation 3 in Lyons et al. 2009 [3]. $I_{45} = I/10^{45}\,\mathrm{g\ cm^2}$ and we follow the conventions of Eq. 6. We will refer to the above derivation as the classical derivation for magnetar dipole radiation. Lyons et al. assume $P = P_o$, using initial period instead and neglecting spindown.

While the classical derivation of a magnetic dipole yields no luminosity when the spin and magnetic axes are aligned, Spitkovksy 2008 [4] derives the time-dependent radiation for a force-free pulsar with a magnetosphere dominated by inertia-free plasma.

$$L_{pulsar} = k_1 \frac{\mu^2 \Omega^4}{c^3}(1 + k_2 sin^2 a), \tag{9}$$

where the cofactors are nearly unity, $k_1 = 1 \pm 0.05$, $k_2 = 1 \pm .01$. Rather, the key difference between Spitkovsky's model and the classical derivation above is that the former not only allows for a magnetar to produce dipole radiation even if its magnetic and rotational axes are aligned, but also allows for more energetic radiation. For maximally misaligned, or orthogonal, axes, Spitkovsky's force-free model allows for magnetar radiation up to twice the classically-derived spindown model. And even when aligned, Spitkovsky's force-free magnetar produces dipole radiation roughly equally to classical magnetars with orthogonal axes. However, when we consider mass-accretion, we will no longer be in the nearly force-free regime and this assumption will no longer be relevant.

2.3 Fallback Accretion and the Propeller Mechanism

We are interested in solving for the magnetar period evolution in the presence of fallback accretion. Thus, we assume a weaker supernova leaving the magnetar in a nonvacuum environment. We will follow Piro and Ott 2011 [1] in the following.

Accretion falls under the magnetar's field influence at the Alfvén radius,

$$r_m = \mu^{4/7} (GM)^{-1/7} \dot{M}^{-2/7}, \tag{10}$$

where μ is the half the magnetar moment, m_o, defined in Section 2.2. The Alfvén radius is derived by calculating the distance from the neutron star where the magnetic field energy density, $B^2/8\pi$ becomes comparable to the kinetic energy density of infalling matter, $1/2\rho v^2$, where ρ is the mass density of the accreting material and v its velocit. We assume the accreting material is in radial free-fall, so the free-fall velocity $v_{ff} = \sqrt{2GM/r}$, where M is the neutron star mass and r the distance of the infalling material from the neutron star. Imposing the continuity equation of mass, $\rho = \dot{M}/(4\pi v_{ff} r^2)$. Setting the ratio of these two energy densities to 1, we get Eq. 10.

Material will corotate with the magnetar up to the cororation radius,

$$r_c = \frac{GM}{\Omega^2}^{1/3}, \tag{11}$$

derived from equating maximal accretion orbital velocity to the Keplerian velocity, $\Omega = \sqrt{GM/R^3}$ in the limit of orbiting material of negligible mass. M is the magnetar mass and R its equatorial radius.

If $r_m > r_c$, infalling material under the influence of the neutron star's dipole field must spin at a super-Keplerian rate to corotate with the neutron star and is thus flung out. If $r_m < r_c$, material will come under the dipole field's influence and corotate with the neutron star at the Keplerian velocity and subsequently be funneled onto the magnetar. This delineates the accretion regime from the propeller regime.

Then, we can solve for the magnetar period dynamics by conserving angular momentum

$$I\frac{d\Omega}{dt} = N_{dip} + N_{acc}, \tag{12}$$

where

$$N_{dip} = -\frac{\mu^2\Omega^3}{6c^3}. \tag{13}$$

We divide N_{acc} into two cases: when $r_m > R$ and and when $r_m < R$. Only in the first case does infalling material come under the dipole field's influence.

We then have

$$N_{acc} = n(\omega)(GMr_m)^{1/2}\dot{M} \text{ for } \mathrm{r_m > R}, \tag{14}$$

where $\omega = (\frac{\Omega}{GM/r_m^3})^{1/2} = (r_m/r_c)^{3/2}$. $n(\omega)$ must be fixed such that N_{acc} is positive, spinning up the magnetar, in the accretion regime $r_m < r_c$ and negative, spinning down the magnetar, in the propeller regime, $r_m > r_c$. Otherwise, if $r_m = r_c$, $n(\omega) = 0$. Following Piro and Ott 2011 [1], we set $n(\omega) = 1 - \omega$. For an Alfven radius internal to the magnetar, $r_m < R$, we have

$$N_{acc} = (1 - \frac{\Omega}{\Omega_k})(GMR)^{1/2}\dot{M} \text{ for } \mathrm{r_m < R}. \tag{15}$$

Infalling material does not come under the influence of the magnetic field before accretion. The prefactor ensures continuity of N_{acc} at $r_m = R$.

The mass accretion rate can be decomposed into early and late times

$$\dot{M}_{early} = \eta 10^{-3} t^{1/2}\,\mathrm{M_\odot s^{-1}}, \tag{16}$$

$$\dot{M}_{late} = 50 t^{-5/3}\,\mathrm{M_\odot s^{-1}}, \tag{17}$$

following Macfadyen et al. 2001 [5] and Zhang et al. 2008 [6]. $\eta \approx 0.1 - 10$ is a dimensionless indicator of the supernova explosion energy. A larger η signifies a weaker explosion energy and hence more fallback. Late-time accretion is independent of explosion energy. Following the convention in Piro and Ott 2011, we combine these expressions

$$\dot{M} = (\dot{M}_{early}^{-1} + \dot{M}_{late}^{-1})^{-1} \tag{18}$$

This has the virtue of returning equation 16 at early times and equation 17 at late times. Other conventions are possible, but for consistency we follow Piro and Ott 2011 [1].

3 Prompt Emission and Magnetic Dissipation

Can fallback accretion increase $\dot{M}$ and hence lower magnetization to allow for longer prompt emission winds? Does the wind direction matter? Metzger 2010 [2]. solves for prompt emission energetics assuming neutrino-driven mass loss (an outflow). Can we similarly account for accreting mass from the supernova (an inflow) in calculationg the magnetization? If not: Following Piro and Ott 2011 [1], there exist certain conditions under which fallback accretion is flung back out. In this propeller regime, we would have mass loss in that sense that mass is flowing outwards from the magnetar, addressing the previous issue. However, compared to Metzger 2010, where neutrino driven mass-loss happens at the surface of the magnetar, the propeller regime occurs at the Alfven radius of ~ 14 km (see Section 2.3). Is this difference significant, given that the internal shock radius responsible for prompt emission is $\sim 10^{13}$ cm and thus much further than both the Alfven radius and the magnetar surface?

3.1 Magnetization and Longevity

3.2 Thermalization: Dissipation vs Shocks

4 Afterglow and Plateau

4.1 Lyons: Spindown Powered Plateau

We explore the argument in Lyons et al. 2009 [3] that plateau features lasting 100s to 1000s of seconds in LGRB afterglows can be explained by the dipole radiation model of a magnetar. As a first order estimate, we trace the steps in Lyons et al. and neglect fallback accretion. Following Piro Ott 2011[1] and neglecting spindown from fallback accretion, we have

$$I\dot{\Omega} = N_{\rm dip}, \tag{19}$$

where we allow for some oblateness $I = 0.35MR^2$[1] and $N_{\rm dip} = -\mu^2\Omega^3/6c^3$. We solve for angular velocity as a function of time

$$\Omega = \frac{\sqrt{\frac{21}{2}}c^{3/2}\sqrt{M}R}{\sqrt{10t\mu^2 - 21c^3MR^2y}}, \tag{20}$$

Together with 5, we can solve for spindown radiation luminosity as a function of time, arriving at

$$L_{\rm dip} = \frac{147B^2c^3M^2R^{10}}{8(-21c^3MR^2y + 5/2B^2R^6t)^2}\ , \tag{21}$$

where we have used $\mu = BR^3/2$, the magnetic moment for a uniformly magnetized sphere, and y is a negative value related to initial period P_o by $P_o = 2\pi\sqrt{-2y}$.

Note the interesting result that luminosity may actually decrease with increasing magnetic field at a given time. A stronger field brakes the magnetar, decreasing its spin frequency as seen in Eq. 20. Since frequency comes in to the inverse 4th power, while the magnetic field comes in only to the 2nd power in Eq. 5, luminosity may indeed decrease with higher magnetic field.

We correct for anistropic emission using Eq. 5 of Lyons et al. 2009 [3]

$$E_{\rm beam} = (1 - \cos\theta_b)E_{\rm iso}\,, \tag{22}$$

where θ_b is the beam's opening angle, and we assumed that this does not change with time. Thus the analogous correlation holds for luminosity.

4.1.1 Assumptions

The assumption in Lyons et al. of $1.4M_\odot$ for the magnetar mass seems troublesome since the non-canonical model demands magnetar collapse to a black hole to shut off the light curve, but $1.4M_\odot$ is a lower limit on NS mass - we do not expect collapse to a BH. However, the requisite near breakup spin may prevent even a short-lived magnetar from forming, allowing immediate NS collapse to BH. Could a similar breakup instability lead to BH collapse for these low mass NS?

We have used Ned Wright's Java Cosmology Calculator for Standard Cosmological Model to arrive at luminosity distances.

The figures below are light curves using data from Swift for LGRB 101225A in the $0.3-10$ keV bandpass.

4.1.2 K-correction

Since GRBs occur at significant redshifts, the source restframe X-ray afterglows are shifted appreciably towards lower frequency bandpasses. We K-correct the detected bandpass into the rest frame of emission as follows. *(include note on comoving vs luminosity distance).* The spectral indices Γ are available from SWIFT at `http://www.swift.ac.uk/xrt_live_cat/`. The spectral index β *(define eqn)* is simply $\Gamma - 1$ and the K-corrected luminosity is then:

$$L_{[.3-10keV]} = 4\pi f_{[.3-10keV]} d_L^2 (1+z)^{-1+\beta} \ , \tag{23}$$

where we use 0.3-10keV as the X-ray bandpass. $L_{[.3-10keV]}$ is the luminosity in this bandpass calculated from the Swift flux data, $f_{[.3-10keV]}$. z is the LGRB redshift and d_L the luminosity distance of the LGRB.

4.2 Centrifugal Support and Black Hole Formation

4.3 Possible Scenarios Involving a Magnetar as GRB Central Engine

- We can have a plateau and apparent cutoff explained entirely by the magnetar dipole curvature. For instance, see Fig 3.

- We can have accretion induced collapse to a blackhole for a variety of magnetar initial masses, from $1.5 - 2.4\, M_\odot$ and a variety of accretion parameters $0.1 - 10$.

- We can have spindown collapse, where centrifugal support is no longer able to sustain the magnetar even in the case of no accretion.

  We may initially have a hypermassive, $> 2.5M_\odot$, differentially rotating magnetar. However, bar mode, magnetic, and other instabilities will redistribute angular momentum to make the magnetar rigidly rotating within the first second. Thus the above collapse arguments still apply (citation needed).

- We may also have no collapse and see an indefinite plateau, or immediate collapse and thus no plateau *(find examples).*

4.4 Fits

We explore the possibity of a magnetar braking until rotational support is insufficent to prevent gravitational collapse.

As an order of magnitude estimate (*why not explore rot. energy vs grav energy*) we plot in Fig. 1 the ratio of the centrifugal force over the gravitational force as a function of magnetar period. Though

the radius may evolve during the first few seconds (see Metzger 2010 [2], it is reasonable to assume that the radius remains constant during the afterglow phase.

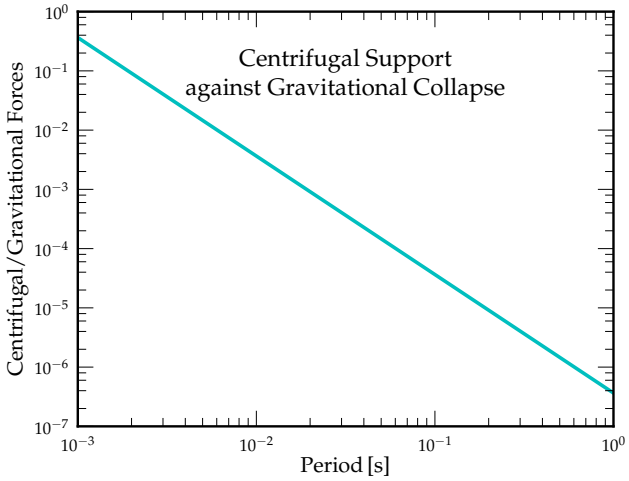

Figure 1

Note how, by a period of a few milliseconds the centrifugal support has become orders less. For context, in Fig. 2 we plot period evolution of magnetars again neglecting fallback and assuming only dipole evolution.

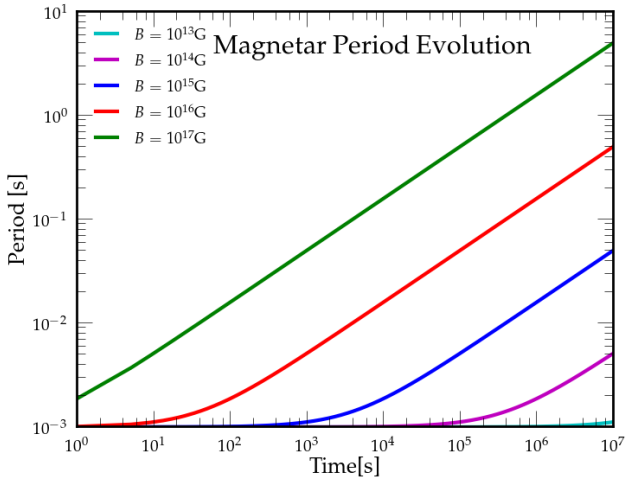

Figure 2

We assume 3.0 solar masses (*cite*) as an upper limit to our magnetar before collapse to a black hole. In Fig. 4, we plot several GRBs against the dipole model for the afterglow phase for a variety of parameters. All assume initial period of 1 ms at the beginning of prompt emission and a radius of 12km. Following Lyons et al., we use small beaming angles of 1° and 4°. The last two plots are fit explicitly rather than constrained by an array of parameters.

Next we consider fallback accretion. In Fig. 3 below, we use the notation rXmYbZ where X is the radius in km, Y is the mass in solar masses and Z indicates the dipole magnetic field in 10^Z Gauss. η is our accretion parameter described above associate with the supernova strength. A smaller η means a stronger supernova and thus less fallback.

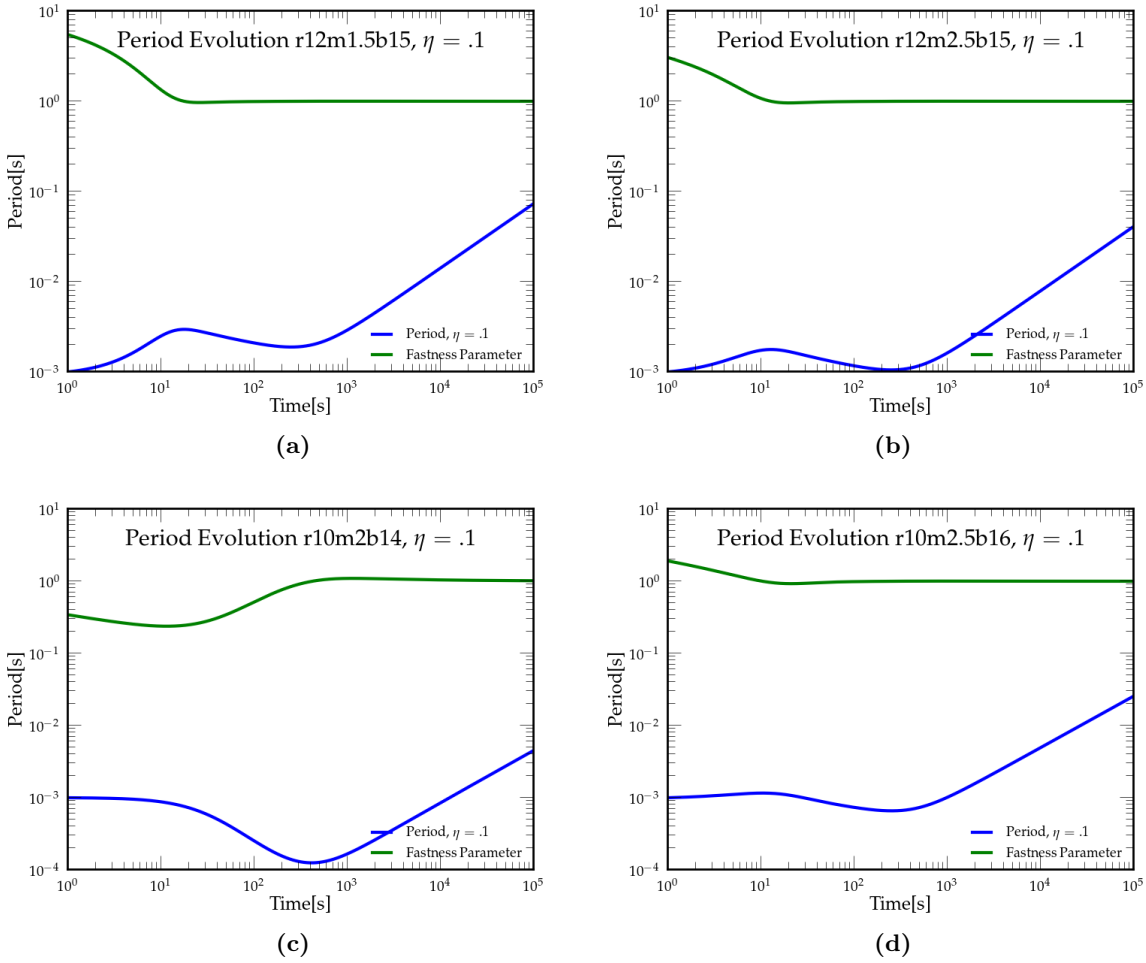

Figure 3

In Figures 3a and 3b, we see that if the magnetar can survive against gravitational collapse for the first 10 seconds, it will power an afterglow lasting up to a 1000 seconds. In Figure 3c, we see the magnetar becomes rotationally unstable around several hundred seconds. In Figure 3d, the magnetar can likely power a plateau of duration greater than 1000 seconds. The fastness parameter plotted is $(r_m/r_c)^(3/2)$ and determines whether the magnetar is in the propeller regime (where the fastness parameter is greater than 1).

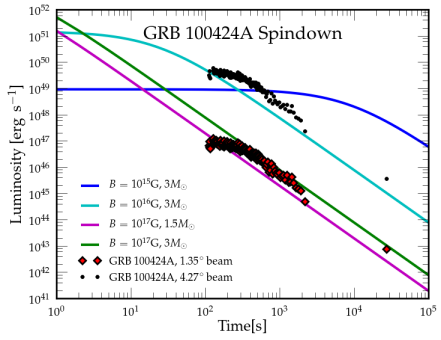

(a) An example of the dipole model alone accounting for both the plateau and decay curvature without the need for a black hole.

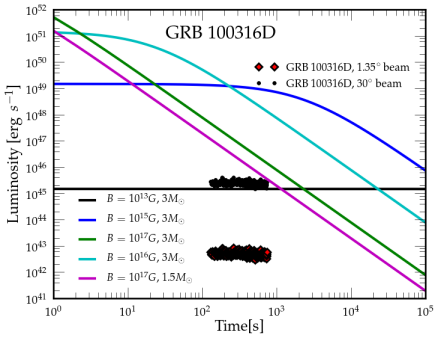

(b) Note that due to the limited data, we cannot extrapolate a beaming angle from the fit.

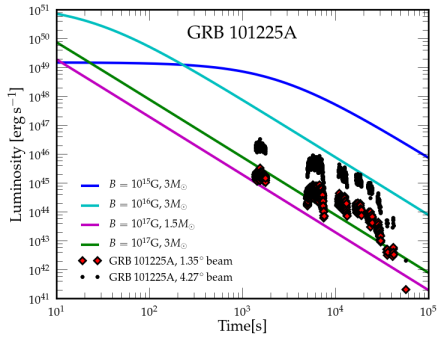

(c) Late time afterglow activity

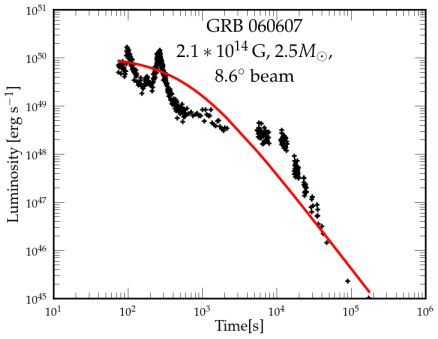

(d) Another example of the dipole model fitting the plateau and decay curvature. The two early peaks are likely flares.

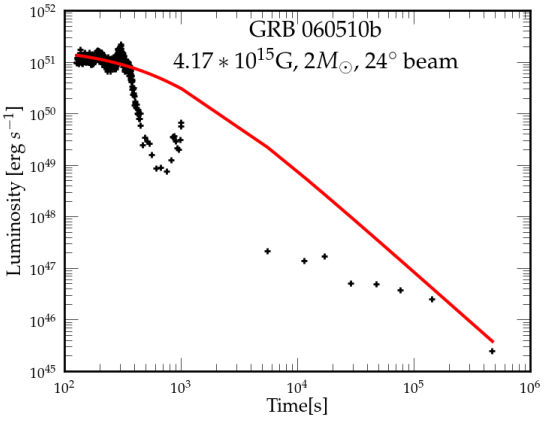

(e) Possible evidence of early decay to a black hole due to the sharp light curve cut-off at 200s with a drop of roughly 2 orders.

Figure 4

At this point we reconsider our assumptions to see if they are self-consistent. We first assume fallback accretion with sufficient material and the absence of apropeller regime. As seen in Fig. 5a, depending on the supernova explosion strength, upwards magnetars may accrete several solar masses M_{odot} in the first several hundred seconds. In Fig. 5b, we plot mass accretion and the fastness parameter for a magnetar with a particularly high 5 ms initial period, initial mass of 2 $M_\odot$ and a field of 10^{15} G. Interestingly, if we decrease the period to 1 ms, the magnetar is always (at least until 10^7 seconds) in the propeller regime and does not accrete. Thus, fallback accretion may play a significant role in magnetars.

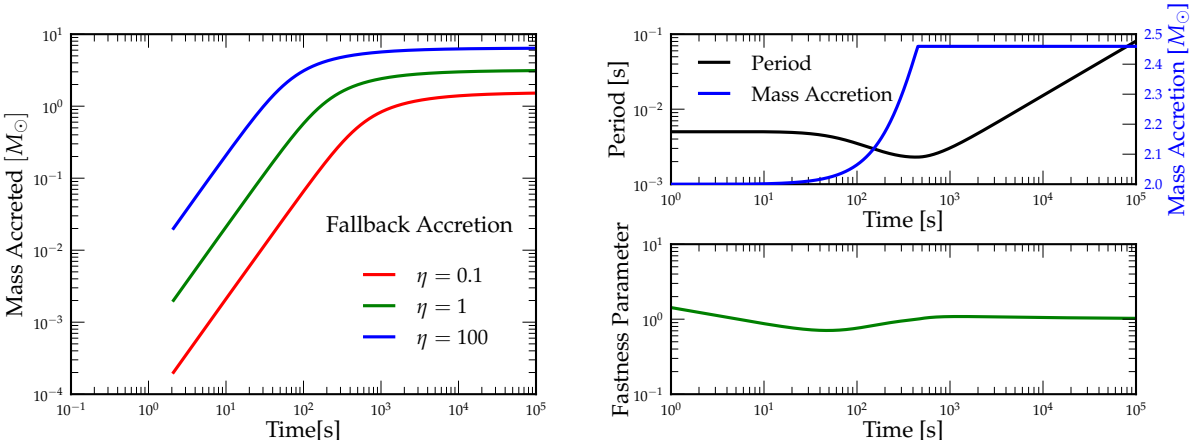

(a) **(b)**

Figure 5

Additionally, we plot in Fig. 6 the ratio of centrifugal to gravitational forces as a function of time and period to determine stability against gravitational collapse.

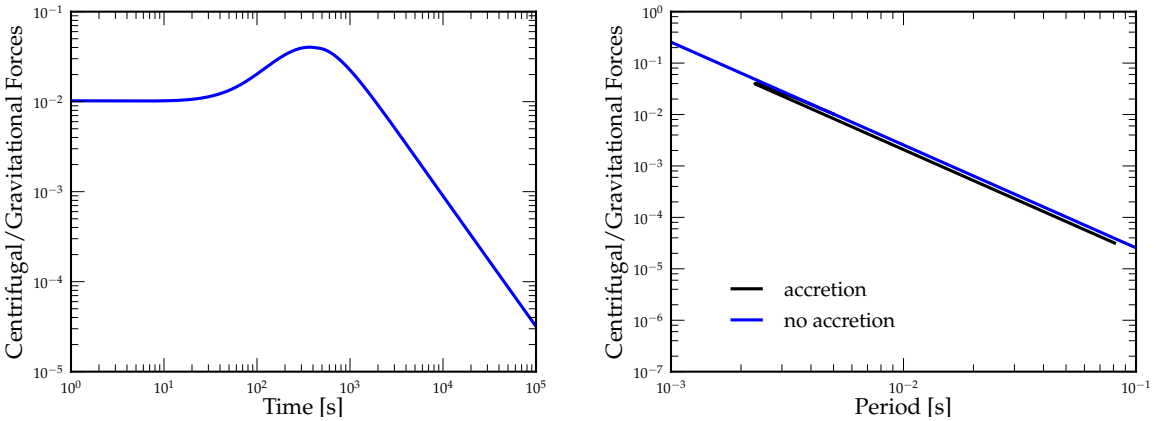

(a) **(b)**

Figure 6

Furthermore, as evident in Fig. 6, period evolution may be deceptive. Though the magnetar has not spun down appreciably even at 1000 seconds, it has by then accreted over 2 $M_\odot$ of material and very likely collapsed even given its rotation (*cite*).

5 Conclusion

6 References

[1] A. L. Piro and C. D. Ott, "Supernova Fallback onto Magnetars and Propeller-Powered Supernovae," *Astrophys.J.* **736** (2011) 108, arXiv:1104.0252 [astro-ph.HE].

[2] B. Metzger, D. Giannios, T. Thompson, N. Bucciantini, and E. Quataert, "The Proto-Magnetar Model for Gamma-Ray Bursts," *MNRAS* **413** (2010) 2031–2056, arXiv:1012.0001 [astro-ph.HE].

[3] N. Lyons, P. O'Brien, B. Zhang, R. Willingale, E. Troja, *et al.*, "Can X-Ray Emission Powered by a Spinning-Down Magnetar Explain Some GRB Light Curve Features?," arXiv:0908.3798 [astro-ph.HE].

[4] A. Spitkovsky, "Time-dependent force-free pulsar magnetospheres: axisymmetric and oblique rotators," *Astrophys.J.* **648** (2006) L51–L54, arXiv:astro-ph/0603147 [astro-ph].

[5] A. MacFadyen, S. Woosley, and A. Heger, "Supernovae, jets, and collapsars," *Astrophys.J.* **550** (2001) 410, arXiv:astro-ph/9910034 [astro-ph].

[6] W.-Q. Zhang, S. Woosley, and A. Heger, "Fallback and Black Hole Production in Massive Stars," *Astrophys.J.* (2007) , arXiv:astro-ph/0701083 [astro-ph].